Magnetic field effect on the terahertz emission from nanometer InGaAs/AlInAs high electron mobility transistors

N. Dyakonova, J. Lusakowski, W. Knap, M. Levinshtein, M. S. Shur, S. Bollaert, A. Cappy

▶ **To cite this version:**

N. Dyakonova, J. Lusakowski, W. Knap, M. Levinshtein, M. S. Shur, et al.. Magnetic field effect on the terahertz emission from nanometer InGaAs/AlInAs high electron mobility transistors. Journal of Applied Physics, 2005, 97, pp.114313-1-5. hal-00125161

HAL Id: hal-00125161
https://hal.science/hal-00125161

Submitted on 25 May 2022

HAL is a multi-disciplinary open access archive for the deposit and dissemination of scientific research documents, whether they are published or not. The documents may come from teaching and research institutions in France or abroad, or from public or private research centers.

L'archive ouverte pluridisciplinaire **HAL**, est destinée au dépôt et à la diffusion de documents scientifiques de niveau recherche, publiés ou non, émanant des établissements d'enseignement et de recherche français ou étrangers, des laboratoires publics ou privés.

Journal of Applied Physics

Magnetic field effect on the terahertz emission from nanometer InGaAs/AlInAs high electron mobility transistors

Cite as: J. Appl. Phys. **97**, 114313 (2005); https://doi.org/10.1063/1.1921339
Submitted: 28 January 2005 • Accepted: 29 March 2005 • Published Online: 27 May 2005

N. Dyakonova, F. Teppe, J. Łusakowski, et al.

View Online Export Citation

ARTICLES YOU MAY BE INTERESTED IN

Terahertz emission by plasma waves in 60 nm gate high electron mobility transistors
Applied Physics Letters **84**, 2331 (2004); https://doi.org/10.1063/1.1689401

AlGaN/GaN high electron mobility transistors as a voltage-tunable room temperature terahertz sources
Journal of Applied Physics **107**, 024504 (2010); https://doi.org/10.1063/1.3291101

Room-temperature terahertz emission from nanometer field-effect transistors
Applied Physics Letters **88**, 141906 (2006); https://doi.org/10.1063/1.2191421

Lock-in Amplifiers up to 600 MHz
Zurich Instruments
Watch

AIP Publishing

© 2005 American Institute of Physics.

HTML ABSTRACT + LINKS

Magnetic field effect on the terahertz emission from nanometer InGaAs/AlInAs high electron mobility transistors

N. Dyakonova, F. Teppe, J. Łusakowski,[a] and W. Knap[b]
Groupe d'Etude des Semiconducteurs (GES)-Unité Mixte de Recherche (UMR) 5650 Centre National de la Recherche Scientifique (CNRS)-Université Montpellier 2, 34900 Montpellier, France

M. Levinshtein
Ioffe Physico-Technical Institute, 26 Polytekhnicheskaya, Saint Petersburg 194021, Russia

A. P. Dmitriev and M. S. Shur
Department of Electrical, Computer, and Systems Engineering and Center for Broadband Data Transfer Science and Technology, CII 9017, Rensselaer Polytechnic Institute, Troy, New York

S. Bollaert and A. Cappy
Institut d'Electronique et de Microélectronique du Nord (IEMN-DHS), Unité Mixte de Recherche, Centre National de la Recherche Scientifique (UMR CNRS) 8520, Avenue Poincaré, 59652 Villeneuve d'Acsq, France

(Received 28 January 2005; accepted 29 March 2005; published online 27 May 2005)

The influence of the magnetic field on the excitation of plasma waves in InGaAs/AlInAs lattice matched high electron mobility transistors is reported. The threshold source-drain voltage of the excitation of the terahertz emission shifts to higher values under a magnetic field increasing from 0 to 6 T. We show that the main change of the emission threshold in relatively low magnetic fields (smaller than approximately 4 T) is due to the magnetoresistance of the ungated parts of the channel. In higher magnetic fields, the effect of the magnetic field on the gated region of the device becomes important. © *2005 American Institute of Physics*. [DOI: 10.1063/1.1921339]

INTRODUCTION

When a direct current flows through a short-channel field-effect transistor, the steady state can become unstable against the generation of high-frequency plasma waves (Dyakonov–Shur instability).[1,2] The transistor channel acts as a resonant cavity for plasma waves and these plasma waves can reach terahertz frequencies for nanosized gate lengths. The excitation of plasma waves with terahertz frequencies was recently successfully demonstrated in heterojunction field-effect transistor with $In_{0.53}Ga_{0.47}As$ channel lattice matched to InP.[3] The terahertz emission reported in Ref. 3 had a threshold character as had been predicted in Refs. 1 and 2. The resonant frequency value and its dependence on the source-drain bias were in a good agreement with the theory.

The design of the heterojunction field-effect transistor, in which terahertz wave radiation was observed in Ref. 3, differed from the one considered by Dyakonov and Shur. The theory was developed for a self-aligned transistor where an entire 2DEG channel was under the gate. The transistor investigated in Ref. 3 had long ungated sections between the source and the gated channel and between the drain and the gated channel. These sections could influence the development of current instability and cause changes of the emission spectrum.[4] In this paper, we demonstrate the dominant effect of the ungated section on the emission behavior in magnetic field.

The transistor studied in Ref. 3 had the source-to-drain length $L_{sd}=1.3$ μm and the gate width was $W=50$ μm. Such an L_{sd}/W ratio should lead to the appearance of the geometrical magnetoresistance[5–7] and the suppression of the negative differential conductivity (NDC).[8]

In this paper, we report on the effect of the magnetic field on the terahertz emission from a heterojunction field-effect transistor of the same design as in Ref. 3 and show that the experimental results are consistent with the plasma instability mechanism of the terahertz emission.

EXPERIMENTAL RESULTS

The active layers of the transistor consisted of a 200-nm $In_{0.52}Al_{0.48}As$ buffer, a 20-nm $In_{0.53}Ga_{0.47}As$ channel, a 5-nm-thick undoped $In_{0.52}Al_{0.48}As$ spacer, a silicon delta-doped layer, a 12-nm-thick $In_{0.52}Al_{0.48}As$ barrier layer, and finally, a 10-nm silicon-doped $In_{0.53}Ga_{0.47}As$ cap layer. The gate length L_g was 60 nm, the source-drain length L_{sd} was 1.3 μm, and the width of the gate was $W=50$ μm. The fabrication details are described in Ref. 9.

The magnetic field B was perpendicular to the plane of the two-dimensional electron gas (2DEG) for $L_{sd}/W=0.026 \ll 1$, i.e., under the condition of a strong geometrical magnetoresistance.[5–7]

The transistor was placed in a cyclotron emission spectrometer designed to perform the spectral analysis of the weak terahertz radiation.[10] The spectrometer consisted of two superconducting coils located one above the other and independently powered. The emitted radiation was analyzed by a magnetically tunable InSb cyclotron resonance detector. The high electron mobility transistor (HEMT) and detector

[a]On leave from: Institute of Experimental Physics, Warsaw University, Hoża 69, 00–681 Warsaw, Poland
[b]Electronic mail: knap@univ-montp2.fr

 © 2005 American Institute of Physics

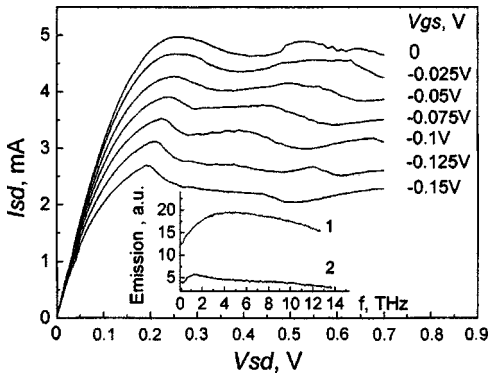

FIG. 1. Output current–voltage characteristics of the InGaAs/AlInAs HEMT. $T=4.2$ K, $B=0$. The inset shows the spectra of emission from the transistor at $V_{sd}=0.6$ V for two values of the gate bias: (1) $V_{gs}=0$ and (2) $V_{gs}=-0.07$ V.

were both placed into a 22-cm-long copper oversized (12-mm diameter) waveguide, so that both of them were in the centers of the coils. The copper waveguide assured total isolation from the background 300 K radiation.

The electron concentration in the channel at the gate voltage $V_{gs}=0$ ($n_0=2.4\times10^{12}$ cm^{-2}) was found from the Shubnikov–de Haas (SdH) measurements. The mobility value in the ungated part of the channel $\mu_0\approx2$ m^2/V s was determined from the geometrical magnetoresistance.

All measurements were carried out at $T=4.2$ K.

The output current–voltage characteristics and the emission spectra of the transistor in the absence of the magnetic field are shown in Fig. 1. The transistor threshold voltage V_{th} was approximately -0.3 V. The gate leakage current did not exceed 1.6×10^{-6} A at $V_{gs}=0$ and 1.7×10^{-4} A at $V_{gs}=-0.15$ V. The NDC was observed at all gate biases. The inset in Fig. 1 shows the terahertz emission spectra measured at $V_{sd}=0.6$ V for two values of the gate bias. The spectra are similar to those observed in Ref. 3, where they were attributed to the plasma-wave emission originating from the region under the gate.

The influence of the magnetic field on the output current-voltage characteristics of the transistor is shown in Fig. 2. This change of characteristics under the magnetic field was typical for all gate biases applied. As seen, the

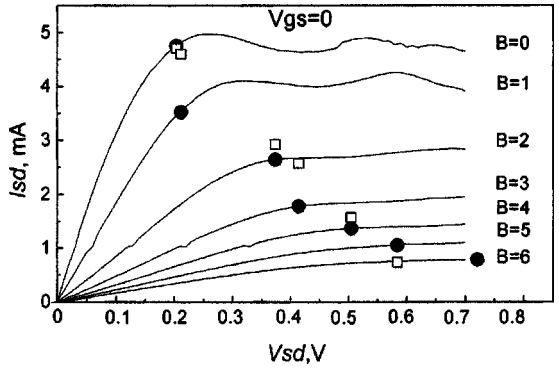

FIG. 2. Current–voltage characteristics at the magnetic field in the range from 0 to 6 T at $V_{gs}=0$. The filled points on the curves mark the threshold of terahertz emission, I_{cr}–V_{cr}. The open squares show the predicted values of emission threshold current (see Discussion section.)

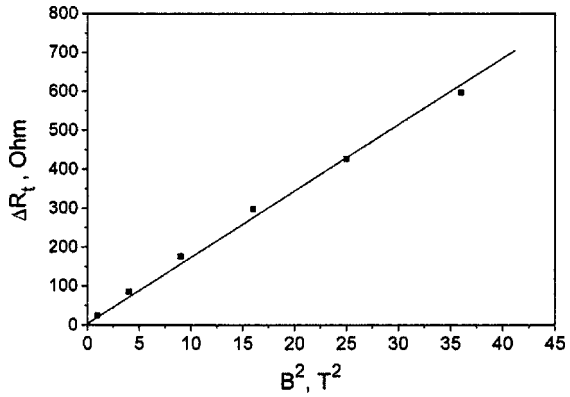

FIG. 3. ΔR_t as a function of squared magnetic field.

saturation voltage V_{sat} increases and the saturation current decreases with a magnetic field B. At $B\geqslant2$ T, the negative differential conductivity at $V_{sd}>V_{\text{sat}}$ disappears. The disappearance of the negative differential conductivity under the magnetic field has been observed in Gunn diodes in Refs. 11 and 12 and explained in the frame of a two-valley model.[13] We also see that both the emission threshold current I_{cr} and the emission threshold voltage V_{cr} depend on magnetic field. Below we will show that these dependencies can be attributed to a strong geometrical magnetoresistance of the ungated regions.

The transistor geometry ($L_{sd}\ll W$) should lead to an increase of the transistor Ohmic resistance in the magnetic field (geometric magnetoresistance). At $V_{gs}=0$, neglecting the contribution of the gated part of the channel to the total resistance $[L_g/(L_{sd}-L_g)\approx0.046]$ we obtain the following equation for geometric magnetoresistance:[5–7]

$$\Delta R_t(B)=R_{sd}(\mu_0 B)^2,$$

where $\Delta R_t(B)=R_t(B)-R_t(0)$, $R_t(0)$ is the total resistance between source and drain at zero magnetic field, $R_t(B)$ is the total resistance in the magnetic field, $R_{sd}=(L_{sd}-L_g)/en_0\mu_0W$ is the resistance of the ungated part of the channel, n_0 is the electron concentration in the ungated part of the channel at $V_{gs}=0$, and μ_0 is the electron mobility in the ungated part of the channel. Figure 3 shows the measured dependence of ΔR_t in the linear regions of current–voltage characteristics on the squared magnetic field at $V_{gs}=0$. As seen, the dependence $\Delta R_t(B^2)$ is linear leading to the mobility value of about 2 m^2/V s. Thus, the effect of the geometric magnetoresistance explains the change of the slope of the linear part of $I_{sd}(V_{sd})$ dependencies. As shown below, the decrease of the saturation current and increase of the drain saturation voltage also results from the same effect.[11,12]

Figure 4 shows the dependence of the terahertz emission intensity on the source-drain voltage at different values of B. During these measurements, the detector integrated the emission signal over the entire emission spectrum.

One can see that the emission versus applied voltage dependence has a threshold character. The emission intensity appears at the threshold voltage V_{cr}, grows, and then saturates. The dependencies are qualitatively the same for all the values of the magnetic field. A general tendency is that the threshold shifts to higher values of V_{sd} and the emission in-

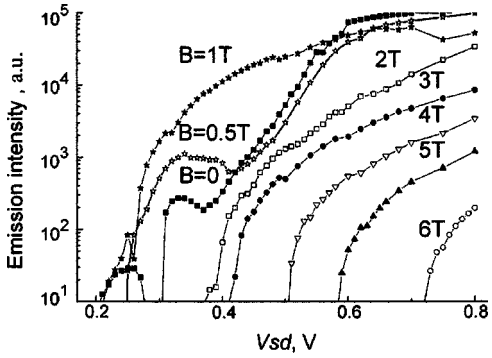

FIG. 4. Emission intensity as a function of the source-drain bias under magnetic field in the range from 0 to 6 T, $V_{gs}=0$.

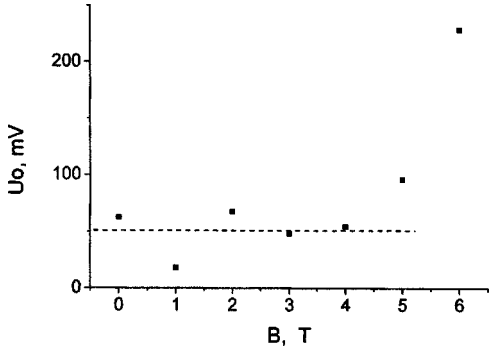

FIG. 5. Voltage drop V_0 across the gated part of the transistor as a function of the magnetic field. The dashed line is an eye guide marking the voltage level of 50 mV.

tensity in the region of the saturation falls when the magnetic field increases. However, we note a peculiar behavior of the emission for magnetic fields smaller than ~1 T. In the absence of the magnetic field, the emission intensity had a small maximum at the source-drain bias near the threshold. At $B=0.5$ T, this maximum becomes more pronounced and at $B=1$ T, it merges with the increasing part of the curve. At $B>1$ T, the whole curve shifts to higher V_{sd}. The origin of this peculiar behavior in small magnetic fields is not clear up to now and requires further investigations. It can be related to the negative differential resistance that is present in low magnetic fields—see Fig. 1. There exists also some possibility that a weak magnetic field can lower the plasma instability threshold voltage/current, due to an increase of the electron transit time in magnetic field.

The threshold voltage of the emission (chosen to correspond to the detector signal of 10 arbitrary units) is indicated in Fig. 2 by filled dots. The value of V_{cr} is close to the saturation voltage of the output characteristics V_{sat}. However, at $B=0$ and 1 T, the terahertz emission starts at voltages smaller than those corresponding to the current saturation and to the NDC region of the current–voltage characteristics. In higher magnetic fields, the emission is still observed, although the NDC disappears. Thus we conclude that the terahertz emission is not related to the NDC.

We estimated the voltage drop across the region under the gate V_0 at the emission threshold using the following equation: $V_{cr}=I_{cr}[R_c+R_{sd}(B)]+V_0$, where R_c is the contact resistance, $R_{sd}(B)=R_{sd}(0)(1+\mu^2B^2)$. The values of $R_c+R_{sd}(B)$, V_{cr}, and I_{cr} were determined experimentally for the values of B from 0 to 6 T and were used to estimate V_0 (see Fig. 5). As seen, the value of V_0 is practically constant ($V_0\approx 0.05$ V) for $B<5$ T, with the exception of the point at $B=1$ T, which corresponds to the nonmonotonic behavior of the emission threshold at this magnetic field. Only at $B\geqslant 5$ T the value of V_0 increases. This effect is explained in the Discussion section.

DISCUSSION

Figure 5 shows that, in moderate magnetic fields (below 4 T), the magnetic field does not affect much the threshold voltage drop across the gated device channel. Based on this fact, we will show that the measured dependencies of the threshold voltage and threshold current of the plasma-wave instability on the magnetic field can be explained by the strong effect of the magnetic field on the ungated sections of the device related to the geometrical magnetoresistance. However, as seen from Fig. 5 and discussed below, in high magnetic fields larger than the critical magnetic field on the order of 4 to 6 T for the device under study, the voltage drop across the channel should become a strong function of the magnetic field.

The effect of the magnetic field on the plasma waves in the gated channel can be described using the following hydrodynamic equations:

$$\frac{d}{dx}\left(-\frac{eV}{m}+\frac{\nu_x^2}{2}\right)=\nu_y\omega_c-\frac{\nu_x}{\tau}, \tag{1}$$

$$\nu_x\frac{d\nu_y}{dx}=-\nu_x\omega_c-\frac{\nu_y}{\tau}. \tag{2}$$

We should notice that the hydrodynamic equations might not be applicable to the ballistic transistor at cryogenic temperatures, since electron–electron collisions are rare under such conditions. However, a relatively large voltage drop across the channel (50 meV) indicates a certain effect of collisions and electron heating in the device channel, which might bring the electron behavior closer to that described by the hydrodynamic equations. The equation for the electron density in the channel follows from the gradual channel approximation $n=C(V_{GT}-V)/e$, and the electron flow per unit device width is given by

$$j=n\nu_x\equiv C(V_{GT}-V)\nu_x/e. \tag{3}$$

Here V is the channel potential, e is the electronic charge, m is the effective mass, ν_x and ν_y are the components of the electron hydrodynamic velocity in the channel, $\omega_c=eB/m$ is the cyclotron frequency, τ is the relaxation time, C is the gate capacitance per unit area, $V_{GT}=V_{GS}-V_{\text{th}}$ is the intrinsic gate voltage swing, and V_{GS} is the intrinsic gate-to-source voltage (i.e., V_{GS} is the voltage drop between the gate and the source side of the gated channel). The x direction is in the direction of the current flow in zero magnetic field, the y direction is along the gate. For a ballistic transistor, $\tau\to\infty$ and Eqs. (1) and (2) become

$$\frac{d}{dx}\left(-\frac{eV}{m}+\frac{\nu_x^2}{2}\right)=\nu_y\omega_c, \tag{4}$$

$$\frac{d\nu_y}{dx}=-\omega_c. \tag{5}$$

The integration of Eq. (5) yields

$$\nu_y=-\omega_c x. \tag{6}$$

Here we assume that the carrier concentration in the ungated regions is very high compared to that in the gate section, and $\nu_y(0)$ is small, where $x=0$ corresponds to the source side of the gated channel. Substituting ν_y from Eq. (6) and V from Eq. (3) into Eq. (4) and integrating the resulting equation yields

$$\frac{e^2 j}{mC\nu_x}+\frac{\nu_x^2}{2}=-\frac{\omega_c^2 x^2}{2}+\text{const}. \tag{7}$$

The voltage drop across a ballistic channel is negligible compared to V_{GT} and V_{sd}, and, to the first order, we can assume that ν_x is constant along the ballistic gated channel, when $B=0$. Therefore, $I\approx V_{sd}/R_{sd}$, where V_{sd} is the extrinsic drain-to-source voltage and R_{sd} is the sum of source and drain series resistances ($R_{sd}=R_s+R_d$), and the electron concentration and hydrodynamic velocities in the channel in zero magnetic field are given by

$$n=CV_{GT}/e, \quad \nu_x=\frac{I}{CV_{GT}W}, \tag{8}$$

respectively. These equations also hold when $m\omega_c^2 L_g^2/2 \ll eV_{GT}$, where L_g is the gate length. We can now introduce a characteristic magnetic field found from the condition $m\omega_c^2 L_g^2/2=eV_{GT}$, and given by

$$B^*=\sqrt{\frac{2mV_{GT}}{eL_g^2}}. \tag{9}$$

For $B\geqslant B^*$, the radius of the electron fluid trajectory becomes comparable to the channel length; the channel resistance should sharply increase. As a result, the magnetic field $B\geqslant B^*$ causes a large voltage drop V_0 across the channel. For the device under study, $m/m_0\sim 0.04$, $V_{GT}\sim 0.1$ V at 3 T, and $L_g\sim 6\times 10^{-8}$ m, leading to $B^*\sim 3.5$ T, in good agreement with the data shown in Fig. 5.

In the magnetic field smaller than B^*, we can neglect the effect of the magnetic field on the potential drop across the channel, and hence, the instability threshold voltage $V_{cr}(B)$ and the threshold current $I_{cr}(B)$ in the magnetic field can be found from the following equations:

$$V_{cr}(B)=V_0+R_{sd}(B)I_{cr}(B), \quad I_{cr}(B)=CV_{GT}\nu_{cr}W. \tag{10}$$

Hence,

$$I_{cr}(B)=C[V_{gt}-I_{cr}(B)R_s(B)]\nu_{cr}W. \tag{11}$$

Here ν_{cr} is the effective electron velocity in the channel at the instability thresholds (which, according to Ref. 2, is on the order of $L/2\tau$, where τ is the electron scattering time). $R_s(B)\approx R_{sd}(B)/2$ is the source series resistance, and $V_0=V_{cr}(L)-V_{cr}(0)$ is the intrinsic emission threshold voltage (shown in Fig. 5). Here $V_{gt}=V_{gs}-V_{\text{th}}$ is the extrinsic gate-to-source voltage swing (V_{gs} being the voltage drop between the gate and source contacts.) Hence, we obtain

$$I_{cr}(B)=C\left[V_{gt}-\frac{V_{cr}(B)-V_0}{2}\right]V_{cr}W. \tag{12}$$

This equation explains the observed decrease of the threshold current with the magnetic field. This decrease is caused by the decrease of the intrinsic gate-to-source voltage $V_{GS}(B)=V_{gs}-V_{sd}(B)-V_0/2$, due to an increase of the voltage drop, $(V_{sd}-V_0)/2$, across the source series resistance caused by the geometric magnetoresistance. The values of I_{cr} predicted by Eq. (12) are shown in Fig. 2 (filled circles.) As seen, the agreement with the measured values is fairly good. The calculations were done for $V_{gt}=0.3$ V and $V_0=50$ mV, using the measured values of $V_{cr}(B)$.

Since the magnetic field decreases the electron concentration in the gated channel, we expect that the peak of the emission spectrum should be redshifted in the magnetic field (see and compare with the insert in Fig. 1). As it is seen in Fig. 2, the integrated signal of emission could be observed at magnetic fields up to 6 T. However, the detector sensitivity was not sufficient to resolve the changes in the emission spectra.

CONCLUSIONS

We have studied the influence of the magnetic field on the excitation of plasma waves in InGaAs/AlInAs lattice matched high electron mobility transistors (HEMTs). The threshold source-drain voltage of the excitation of the terahertz emission shifted to higher values and the instability threshold current decreased with the magnetic field increasing from 0 to 6 T.

The observed terahertz emission persists when the negative differential conductivity is suppressed by the magnetic field, and hence, it is not related to the negative differential conductivity region.

This increase of the threshold voltage and the decrease of the threshold current in magnetic fields below 4 T are explained in terms of the geometrical magnetoresistance of long ungated sections of the transistor. It is shown that at least up to 4 T the parameter that controls the plasma excitation threshold is the voltage drop across the gated region of the transistor. The hydrodynamic model predicts that magnetic fields higher than a critical magnetic field should strongly affect the plasma waves in the gated channel. This predicted critical value is consistent with the measured value of the magnetic field at which the voltage drop across the gated channel significantly increases.

ACKNOWLEDGMENTS

The work at Rensselaer Polytechnic Institute was supported by the National Science Foundation (Project Monitor: Dr. James Mink). At Ioffe Institute this work was supported by the Russian Foundation for Basic Research. We would like to thank M. Dyakonov and V. Kachorovski for kind attention to our work and useful discussions. The research at Montpellier2 University was supported by ACI "Tera-Nano,"

by the French Ministry of Scientific Research, and by the CNRS research group (GdR) "Solid State Detectors and Emitters of Terahertz Radiation."

[1]M. Dyakonov and M. S. Shur, Phys. Rev. Lett. **71**, 2465 (1993).
[2]M. Dyakonov and M. S. Shur, in *Terahertz Sources and Systems*, edited by R. E. Miles (Kluwer Academic, Dondrecht, 2001), p. 187.
[3]W. Knap, J. Łusakowski, T. Parenty, S. Bollaert, A. Cappy, V. V. Popov, and M. S. Shur, Appl. Phys. Lett. **84**, 2331 (2004).
[4]A. Satou, I. Khmyrova, V. Ryzhii, and M. S. Shur, Semicond. Sci. Technol. **18**, 460 (2003).
[5]M. E. Levinshtein and S. L. Rumyantsev, Fiz. Tekh. Poluprovodn. (S.-Peterburg) [Sov. Phys. Semicond. **17**, 1176 (1983)].
[6]M. H. Song, A. N. Birbas, A. van der Ziel, and A. D. van Rheenen, J. Appl. Phys. **64**, 727 (1988).
[7]Y. M. Meziani *et al.*, J. Appl. Phys. **96**, 5761 (2004).
[8]V. B. Gorfinkel' and M. E. Levinshtein, Phys. and Tech. Semicond. **14**, 1694 (1980).
[9]T. Parenty, S. Bollaert, J. Mateos, X. Wallart, and A. Cappy, Proceedings of the Indium Phosphide and Related Material (IPRM) Conference, Nara, Japan, May 2001 (unpublished), p. 626
[10]W. Knap, D. Dur, A. Raymond, C. Meny, J. Leotin, S. Huant, and B. Etienne, Rev. Sci. Instrum. **63**, 3293 (1992).
[11]M. E. Levinshtein, D. N. Nasledov, and M. S. Shur, Phys. Status Solidi **33**, 897 (1969).
[12]M. E. Levinshtein, T. V. L'vova, D. N. Nasledov, and M. S. Shur, Phys. Status Solidi A **1**, 177 (1970).
[13]D. E. McCumber and A. G. Chynoweth, IEEE Trans. Electron Devices **13**, 4 (1996).